RESEARCH ARTICLE

Applied Organometallic Chemistry **WILEY**

Green preparation of bract extract (*Musa acuminate*) doped magnesium oxide nanoparticles and their bioefficacy

Jayashree Shanmugam[1] | Aruna Sharmili Sundararaj[1] |
Roshitha Shanmugasundaram[1] | Balaji Ravichandran[2] |
Mahendrakumar Mani[3] | Savaas Umar Mohammed Riyaz[4,5] |
Manikandan Dhayalan[6] | Antonio Cid-Samamed[7] | Jesus Simal-Gandara[8]

[1]Department of Biotechnology, Stella Maris College (Autonomous), Chennai, 600 086, India

[2]Centre for Advanced Study in Botany, University of Madras, Chennai, 600 025, India

[3]Department of Biotechnology, Guru Nanak College (Autonomous), Chennai, 600 042, India

[4]PG & Research Department of Biotechnology, Islamiah College (Autonomous), Vaniyambadi, Tamil Nadu, 635752, India

[5]Department of Prosthodontics, Saveetha Dental College & Hospitals, Saveetha Institute of Medical and Technical Sciences (Saveetha University), Chennai, Tamilnadu, 600 077, India

[6]Small Molecules and Drug Discovery Group, Anticancer Bioscience, Tianfu International Biotown, Chengdu, 610000, China

[7]Department of Physical Chemistry, Faculty of Sciences, University of Vigo, Ourense, E-32004, Spain

[8]Department Analytical Chemistry and Food Science, Faculty of Science, Universidade de Vigo, Nutrition and Bromatology Group, Ourense, E-32004, Spain

Correspondence
Aruna Sharmili S., Department of Biotechnology, Stella Maris College (Autonomous), Chennai 600 086, India.
Email: arunasharmili@stellamariscollege.edu.in

Manikandan Dhayalan, Small Molecules and Drug Discovery Group, Anticancer Bioscience, Tianfu International Biotown, Chengdu 610000, China.
Email: manikandandhayalan88@gmail.com

Jesus Simal-Gandara, Department of Analytical Chemistry and Food Science, Faculty of Science, Universidade de Vigo, Nutrition and Bromatology Group, E-32004 Ourense, Spain.
Email: jsimal@uvigo.es

Magnesium oxide nanoparticles (MgONPs) synthesized by efficient green approach have unique physiochemical properties. In this study, MgONPs are synthesized with bract extract of *Musa acuminate*, an agro waste. The surface plasmon resonance at 450 nm in UV spectrum and FTIR peaks at 601 and 890 cm^{-1} confirmed the presence of MgONPs. XRD pattern revealed high crystallinity of the nanoparticles with an intense orientation peak at 111, and the size was 13 nm. The particles were spherical with an average size of 24.85 nm. The elemental percentage of magnesium and oxygen were 68.55% and 31.45%. MgONPs had antibacterial activity against *Bacillus subtilis*, *Escherichia coli*, *Vibrio harveyi*, *Vibrio parahemolyticus*, and *Staphylococcus aureus* with MIC, 6 μg/mL. The IC_{50} value for MCF-7 cell was 113.56 μg/mL, and the normal cell line was 785.69 μg/mL. The NPs also exhibited hemolytic features in a dose-dependent manner. The MgONPs exhibited photocatalytic degradation of methyl violet, CBB G-250, and malachite green in 60 min duration. MgONPs had promising antibacterial, cytotoxic, hemolytic, photocatalytic, and seed germination activity. They have the potential to serve as an additive in a variety of biological applications.

KEYWORDS

agro-waste, biological synthesis, MCF-7 cells, photocatalytic activity, seed germination

1 | INTRODUCTION

Nanotechnology has emerged as a multidisciplinary field, expanding its application to biomedicine, tissue engineering, pharmaceuticals, catalysis, electronics, energy harvesting, mechanical industry, environment, material science, cosmetics, and food technology.[1,2] Nanoparticles (NPs) can be obtained using two methods: top-down and bottom-up.[3] Various methods for synthesizing nanoparticles (NPs) are employed, namely, physical, chemical, electrochemical, and biological.[4,5] Physical and chemical methods involve toxic and expensive chemicals and are not environmentally friendly.[6,7] In this regard, current research is focused on biological methods for the synthesis of NPs by the use of plants, plant products, and microorganisms from metal and metal oxides, which are more advantageous as it is cost-effective, safe, environmentally friendly, clinically adaptable, and bio-compatible instead of using hazardous chemicals and extreme reaction conditions.[8–10] Metal and metal oxide nanoparticles have wide applications as catalysts, conductors, biosensors, cytotoxic agents, antimicrobial drugs, and diagnostic tools due to their high dispersion properties in solution and surface-to-volume ratio.[11,12] Numerous metal and metal oxide NPs have been generated using plant biomass due to their high yield, renewability, and availability.[13] Plants are the most common biological substrate for NPs synthesis as they are simple, easy, and safe to handle compared with microbes.[8] Plant parts such as leaves, flowers, fruits, roots, barks, fruit peel, and pulp synthesize NPs.[14] Plants contain various biomolecules such as phenols, alkaloids, flavonoids, terpenoids, proteins, amino acids, enzymes, and vitamins that effectively reduce, cap, and stabilize chloride and nitrate precursors for biosynthesis of NPs.[1,15,16] Thus, they act as stabilizers and reductants.[17] Plant extract natural antioxidants help scavenge reactive oxygen species (ROS), free radicals, and chelate metal ions. In addition, the green route synthesis generates well-defined NPs with definite shapes and size.[18] Plant-mediated NPs find enormous application in medicine as anti-inflammatory, antioxidant antibacterial, antifungal, anticancer, and antiangiogenic agents.[19] Many plants have been used in the synthesis of NPs, such as *Saussurea costus*, *Manilkara zapota*, *Cynara scolymus*, *Annona squamosa*, *Ziziphora clinopodioides*, *Magnolia cobus*, *Falcaria vulgaris*, *Aloysia citrodora*, *Cassia alata*, *Lavandula angustifolia*, and *Argyreia nervosa*.[19–21]

Unique biocompatibility, high stability under extreme conditions, and distinctive physiochemical properties make magnesium oxide nanoparticles (MgONPs) eco-friendly, economically feasible, and industrially important.[22,23] Biomolecules present in plant extracts reduce Mg^+ ions to Mg^0 valency state.[24,25] Among the metal oxide NPs, MgONPs have versatile applications, including catalysis, ceramics, electronics, additives, paints and phytochemical products[26] heavy metal detection and removal, pesticide degradation, and dye removal.[27,28] Properties such as high strength-to-weight ratio, hygroscopic nature, low density, recycling activity, good functionality, and nontoxicity make MgONPs promising biological implants.[29] They possess a unique combination of biocompatibility, biodegradation, and intrinsic fluorescence, making them applicable in cutting-edge fluorescence-guided surgery.[30] Moreover, these NPs exhibit excellent toxic effects against multidrug-resistant human pathogens as protein caps on the metal NPs stabilize the bacterial cell surface, enhancing the binding and absorption of drugs by the infected cells, and hence can be used as an alternative medication. They are used as ointments to treat wounds and burns.[31]

Metal oxide NPs find their way as anticancer therapeutic agents and are used in proof-of-principal nanocryo surgery for cancer treatment.[31–33] Human serum albumin-doped MgONPs have exhibited anticancer activity against leukemia K562 cell lines.[34] Similarly, MgONPs prepared with curcumin and beta-cyclodextrin efficiently kill breast cancer cells (MCF-7).[35] Recently, research has been reported on MgONPs from various plant extracts such as neem leaves, Parthenium, rind of *Punica granatum*, *Manihot esculanta*, *Aloe vera*, *Rosarinus officinalis*, *Pterocarpus marsupium*, *Brassica oleracea*, *Trachyspermum ammi*, and *Camellia sinensis*.[36–41] Despite this, more plants need to be explored to synthesize green NPs. Hence, this work explored the biomedical efficacy of the flower bract generated as an agro waste. *Musa acuminate* Colla. is a wild species of banana plant found in tropical and subtropical regions. The plant parts, including leaves, flowers, pseudostem, corn, fruits, peels, and sap, are used in traditional medicine to treat various illnesses.[42] Considering the uninterrupted availability of this agro-waste and the medical importance of MgONPs, the current work was undertaken to synthesize MgONPs using a bract extract of *Musa acuminata* Colla. flowers and study the antibacterial, cytotoxic, hemolytic, and photocatalytic activities besides testing its efficacy on seed germination.

2 | MATERIALS AND METHODS

2.1 | Materials

Musa acuminata Colla. bract was collected from agricultural land in Mettupalayam, Coimbatore District, Tamil Nadu, and identified. Magnesium chloride (MgCl₂), 3-(4,5-dimethythiazol-2-yl)-2,5-diphenyl tetrazolium bromide (MTT), Dulbecco's modified Eagle medium (DMEM), and fetal bovine serum (FBS) were obtained

from Himedia. The bacterial strains used were *Bacillus subtilis* (ATCC6633), *Escherichia coli* (ATCC25922), *Staphylococcus aureus* (ATCC25923), *Vibrio harveyi* (ATCC33843), and *Vibrio parahaemolyticus* (ATCC17802).

2.2 | Methods

2.2.1 | Preparation of plant extract

Musa acuminata Colla. bract, commonly known as red banana bract was used for the synthesis of MgONPs. The bract was washed thoroughly, shade-dried for 3–4 days, chopped into pieces and stored. To prepare the bract extract, 5 g of the processed sample was mixed in 100 mL of deionized water and heated at 65°C for 30 min. It was then cooled, filtered at room temperature, and used for NPs synthesis.[43]

2.2.2 | Optimization of synthesis parameters

Based on molarity, pH, temperature, and concentration ratio (salt solution:plant extract), the synthesis process was optimized as shown in Table 1.

2.2.3 | Synthesis of MgONPs

To 90 mL of 0.1 M $MgCl_2$ solution, 10 mL of the prepared plant extract was added drop by drop with swirling. The pH was adjusted to 12 using a 2 M NaOH solution. The mixture was kept in a magnetic stirrer and heated at 80°C for 15 min. The formation of a white-colored precipitate indicates the end-point of the synthesis of MgONPs. The solution was centrifuged at 5000 rpm for 15 min, and the white precipitate obtained was washed with sterile distilled water twice and air dried.[44]

2.2.4 | Characterization

As a primary screening step, the plasma resonance of MgONPs was analyzed by a double beam spectrophotometer (WSP-UV-580PC) in the 200–800 nm range. The

possible functional molecules responsible for the reduction and capping of the prepared MgONPs are identified by Fourier transform infrared spectroscopy (FTIR) with a DTGS detector (Bruker). The samples were prepared by mixing the generated MgONPs with potassium bromide (KBr) powder to form thin translucent discs. The transmittance was recorded in the range of 400–4000 cm^{-1} with a set resolution of 4 cm^{-1}. The crystalline structure of synthesized MgONPs was studied by X-ray diffraction studies (powder X-ray diffractometer-P Analytical, Xpert3). The purity and crystalline size of the NPs were determined at 40 kV with a current of 30 mA using Cu Kα radiation using a diffractometer. The Debye–Scherrer formula calculated the average size of the NPs:

$$D = 0.91\lambda/(\beta\cos\theta).$$

where D corresponds to the crystalline size, 0.9 is Scherrer constant, $\lambda = 1.5406$ Å, β is full width with half maximum (FWHM) of the most intense peak and θ is the Braggs diffraction angle.[19] Scanning electron microscopy (SEM) (FEI Quanta 200F) was used to study the surface morphology using secondary electrons and backscattered electron mode at an accelerating voltage of 20 kV. Energy dispersive X-ray (EDX) was done to analyze the elemental composition.[45]

2.2.5 | Antibacterial assay

The antibacterial activity of the synthesized MgONPs was determined by assessing the Minimum Inhibitory concentration (MIC) against *Bacillus subtilis* (ATCC 6633), *Escherichia coli* (ATCC 25922), *Staphylococcus aureus* (ATCC 25923), *Vibrio harveyi* (ATCC 33843), and *Vibrio parahaemolyticus* (ATCC 17802). A stock was prepared by dissolving 30 mg of the MgONPs in 5 ml deionized water. Using saline, the bacterial cultures in the log phase were adjusted to 0.5 McFarland standard (1.5×10^{-8} CFU/mL). A primary volume of MgONPs was added to get various concentrations (6, 3, 1.5, 0.75, and 0.375 μg/mL). Then 100 μL of bacterial inoculum was added to the wells of a microtiter plate accordingly. Positive and negative control wells were also maintained. Negative control consists of test organisms and saline,

TABLE 1 Optimization of various parameters for synthesis of MgONPs.

Concentration of $MgCl_2$	1 mM	5 mM	10 mM	50 mM	100 mM
pH	7	8	9	10	12
Temperature	40	50	60	70	80
Concentration ratio Salt solution:plant extract	5:5	6:4	7:3	8:2	9:1

whereas the positive control has saline and streptomycin solution. The microtiter plate was incubated at 37°C for 24 h aseptically. The percentage of inhibition was measured and recorded using plate reader at 495 nm.[46]

2.2.6 | In vitro cytotoxicity assay

The synthesized MgONPs were evaluated for antiproliferative activity against the breast cancer cell line (MCF-7), and cytotoxicity was tested on Vero cell line. The percentage of cell viability was determined by colorimetric assay, using 3-(4,5-dimethythiazol-2-yl)-2,5-diphenyl tetrazolium bromide (MTT) and compared with untreated controls. The cells were seeded in 96-well plates in 100 μL of medium (DMEM) containing 5% FBS, with a density of 10,000 cells per well and incubated at 37°C with 5% CO_2 prior to the addition of MgONPs. After the cells were attached, different concentrations of MgONPs (10–100 μg) were added and incubated at 37°C with 5% CO_2 and 95% oxygen. Triplicates were maintained and the wells without the sample served as control. After 48 h, 50 μL of MTT (5 mg/mL) in phosphate buffer saline (PBS) was added to each well and incubated at 37°C for 4 h. Then 100 μL of dimethylsulfoxide (DMSO) was added to the medium to solubilize the formazan crystals. Absorbance was measured at 570 nm using microplate reader.[47] The percentage of cell viability was determined using the following formula:

$$Percentage\ of\ inhibition\ (\%) = 100 - \frac{Absorbance\ (Sample)}{Absorbance\ (control)} \times 100$$

2.2.7 | In vitro hemolytic activity

Fresh heparinized human blood was collected and washed thrice with PBS (pH -7.4) by centrifuging at 1000 rpm for 10 min to separate the plasma. The obtained pellet containing the red blood cells (RBCs) was resuspended in 20 mL of PBS. Two hundred micrograms of MgONPs were dissolved in 1 mL PBS. The RBC suspension was treated with an equal volume of MgONPs of various concentrations (100, 50 25, 12.5, 6.25, and 3.125 μg/mL) and incubated at 25°C for 30 min. The RBCs treated with Triton X-100 (2%) and PBS (pH 7.4) were used as the positive and negative control, respectively. After incubation, the mixture was centrifuged at 1000 rpm for 5 min, and the absorbance of the supernatant was measured at 540 nm using plate reader.[48] The

percentage of hemolysis was calculated by the following formula:

$$Percentage\ of\ Hemolysis = 100 \times \frac{Abs.of\ Sample - Abs.of\ PBS}{Abs.of\ Triton\ X - Abs.of\ PBS}$$

where Abs denotes absorbance.

2.2.8 | Photocatalytic activity

Photocatalytic activity of biosynthesized MgONPs was studied by the degradation of organic dyes such as methyl violet, Coomassie brilliant blue G-250, and malachite green. Twenty micrograms of MgONPs were added to 10 mL of dye solution. Treatment without NPs served as control. The reaction mixture was kept dark for 1 h and then placed under direct sun irradiation. The absorbance was recorded at regular intervals until the solution turned colorless. The following formula calculated the percentage of decolorization:

$$Percentage\ of\ decolorization = \frac{C_0 - C}{C_0} \times 100$$

where C_0 is the initial concentration of the dye solution and C is the concentration of dye solution after photocatalytic degradation.[49]

2.2.9 | Seed germination

The green-synthesized MgONPs were used to investigate the effect of seed germination using the seeds of *Vigna radiata* (Green gram). The seeds were surface sterilized using 70% ethanol, Tween20, mercuric hypochlorite, and deionized water. The sterilized seeds were soaked in deionized water for 3 h. Healthy seeds were then immersed in MgONPs suspension for 2 h. The seeds were then transferred onto absorbent cotton containing deionized water. The set-up was maintained under the aseptic condition at room temperature. The germination was monitored at regular intervals.[50]

2.3 | Statistical analysis

The data collected on the various parameters for this experimental study were analyzed.

The mean ± standard deviation of three independent readings was used to express the values.

3 | RESULTS AND DISCUSSION

Different factors like the pH, temperature, volume of the plant extract, and the molarity of $MgCl_2$ solution were modified to obtain the NPs. Based on all the parameters analyzed the ratio of 9:1 (salt solution:extract) exhibited a color change from colorless to a typical dark brown color. This color change after 15 min of interaction indicated the formation of MgONPs, whereas the other vials did not give rise to the desired color change nor exhibited the spectral properties that correspond to that of MgONPs. Thus, the MgONPs with desirable properties were synthesized using bract extract of *Musa acuminata* bract as a bio-reductant at pH 12, using 100 mM salt concentration at a temperature of 80°C.

3.1 | Characterization

3.1.1 | UV–visible spectrometer analysis

The shape, size, and distribution of NPs in the colloidal matrix influence the surface plasma resonance (SPR) band. The SPR pattern depends on the size, the shape of the metal particles, and the dielectric properties of the medium used to synthesize the NPs, stabilizing molecules on the surface of the NPs.[51,52] A single plasma resonance peak at 385 nm for MgONPs was observed upon spectrometric analysis (Figure 1), which confirmed the reduction of Magnesium chloride to MgONPs.

The SPR absorption may be due to the interaction of free electrons of the MgONPs and the light wave.[53] According to Mie's theory, spherical nanoparticles show only a single SPR band, whereas anisotropic particles show two or more SPR bands depending on the shape of the NPs.[54,55] The single peak in the UV–Vis spectrum indicates the prepared nanoparticles were iso-morphological.[56] Phytochemical constituents such as alkaloids, tannins, phenols, and flavonoids in the bract extract act as bio-reducing agents resulting in the formation of MgONPs.[57] They attune the morphology, surface chemistry, shape and size, and minimize the agglomeration/aggregation of the NPs.[58] The capping agents regulate the stability and functionalization of the NPs in the medium in which they are suspended.[59] A similar pattern of SPR behavior in the range of 300–400 nm was reported for MgONPs by previous researchers.[1,9,43]
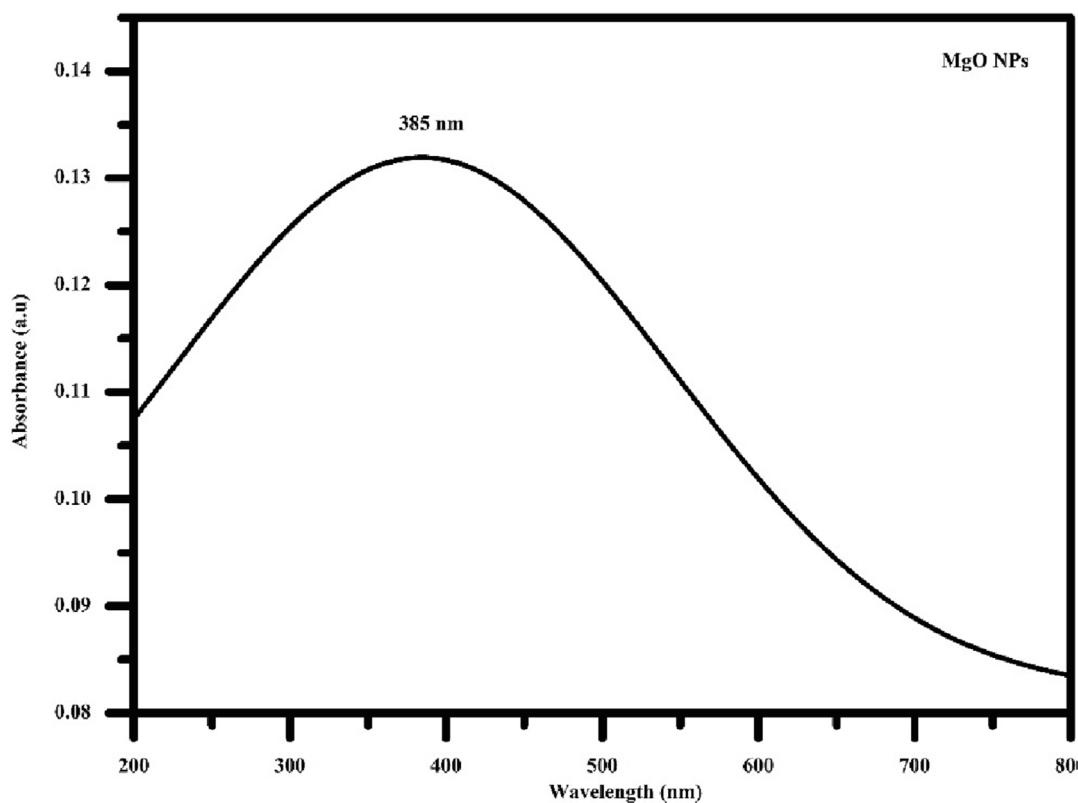

FIGURE 1 UV–Vis spectra of magnesium oxide nanoparticles (MgONPs) synthesized using the bract extract of *Musa acuminata* flower.
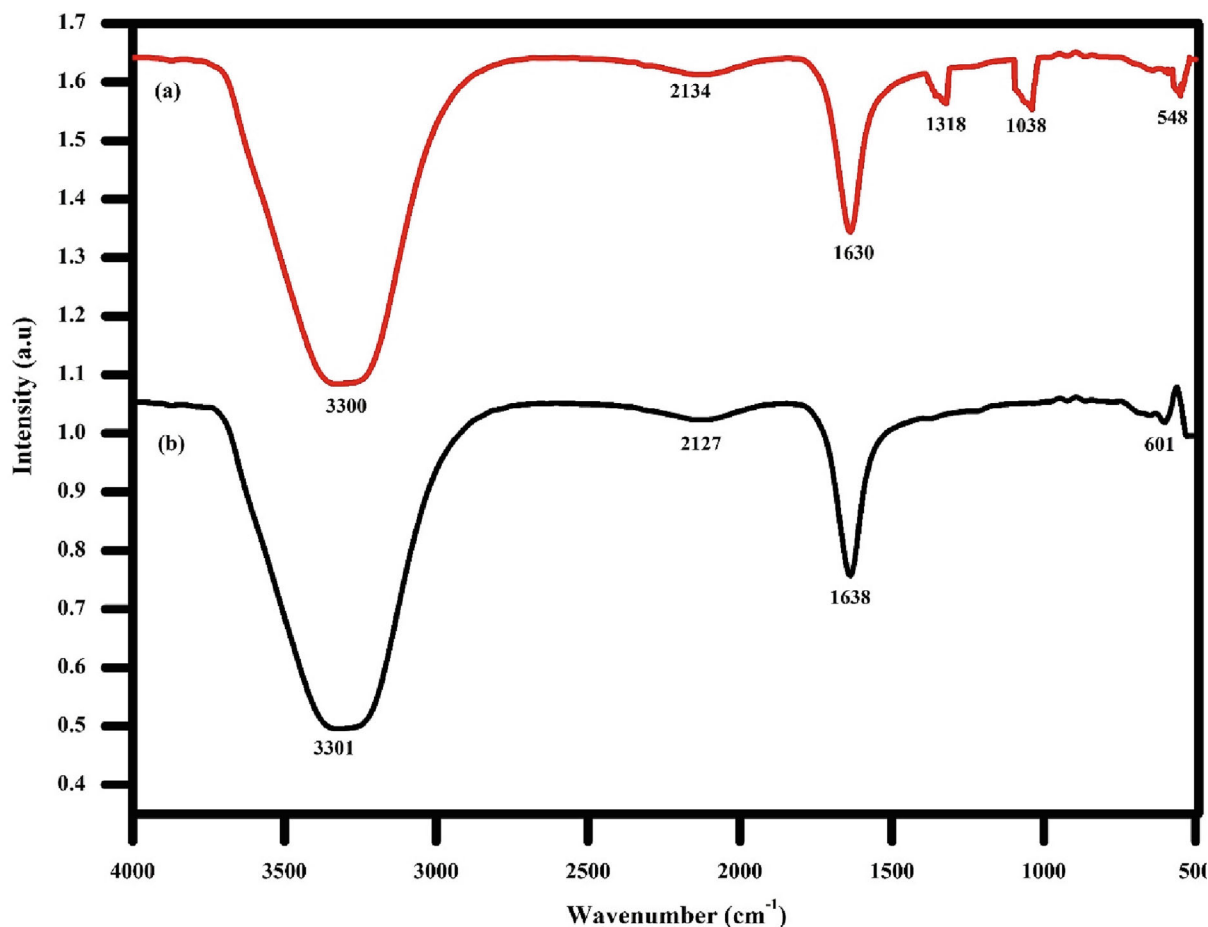
FIGURE 2 FT-IR spectrum of (a) bract extracts of *Musa acuminata* flower; (b) MgONPs.

3.1.2 | Fourier transform infrared spectroscopy (FT-IR)

FTIR analysis was performed for wave number VS transmittance in the scan range of 500–4000 cm^{-1} to identify the interactions of synthesized MgONPs using bract extract of *Musa acuminata* (Figure 2).

FT-IR spectra of MgONPs exhibit a broad peak at 3301 cm^{-1} (OH stretching), 2127 cm^{-1} (C≡C—; alkyne stretching), and 1638 cm^{-1}(C=O stretching) and found that the stretching vibration mode in the range of 601 and 890 cm^{-1} indicates the formation of Mg—O—Mg bonds.[60,61] Molecules that contain the functional group —C—O—C, —C—O—, —C≡C—, and —C=O— have been reported to act as reducing agents in green synthesis.[62] The marginal shift in the peak position and absence of a few peaks indicate plant compounds acting as reducing agents.[1]

3.1.3 | XRD analysis

XRD analysis of MgONPs (Figure 3) showed significant peaks at 37.1°, 42.4°, 62.5°, 74.7°, and 78.70°, respectively,

representing (111), (002), (200), (113), and (222) planes, indicating the formation of the polycrystalline structure of MgONPs. The results are in agreement with International Center for Diffraction Data Card (JCPDS No. 87-0653).[60] XRD pattern shows an intense orientation peak (111), revealing the high crystallinity of the synthesized NPs. The size of the NPs calculated by the Debye–Scherrer formula was 13 nm. The few peaks in the spectrum indicate the lack of metallic impurities.[9]

3.1.4 | SEM–EDX

The surface morphology of the green synthesized MgONPs and the quantitative chemical composition were investigated by SEM–EDX. The SEM images showed spherical MgONPs with an average size of 24.85 nm (Figure 4a,b). SEM images show the sizes of the metallic core of the particle and also the particle size accuracy scales with the SEM image resolution.[63] The small average size of the NPs plays an important role in antibacterial activity; the smaller the size, the greater the antibacterial activity.[64] The EDX profile contains Mg and O with a weight percentage of 68.55% and 31.45%
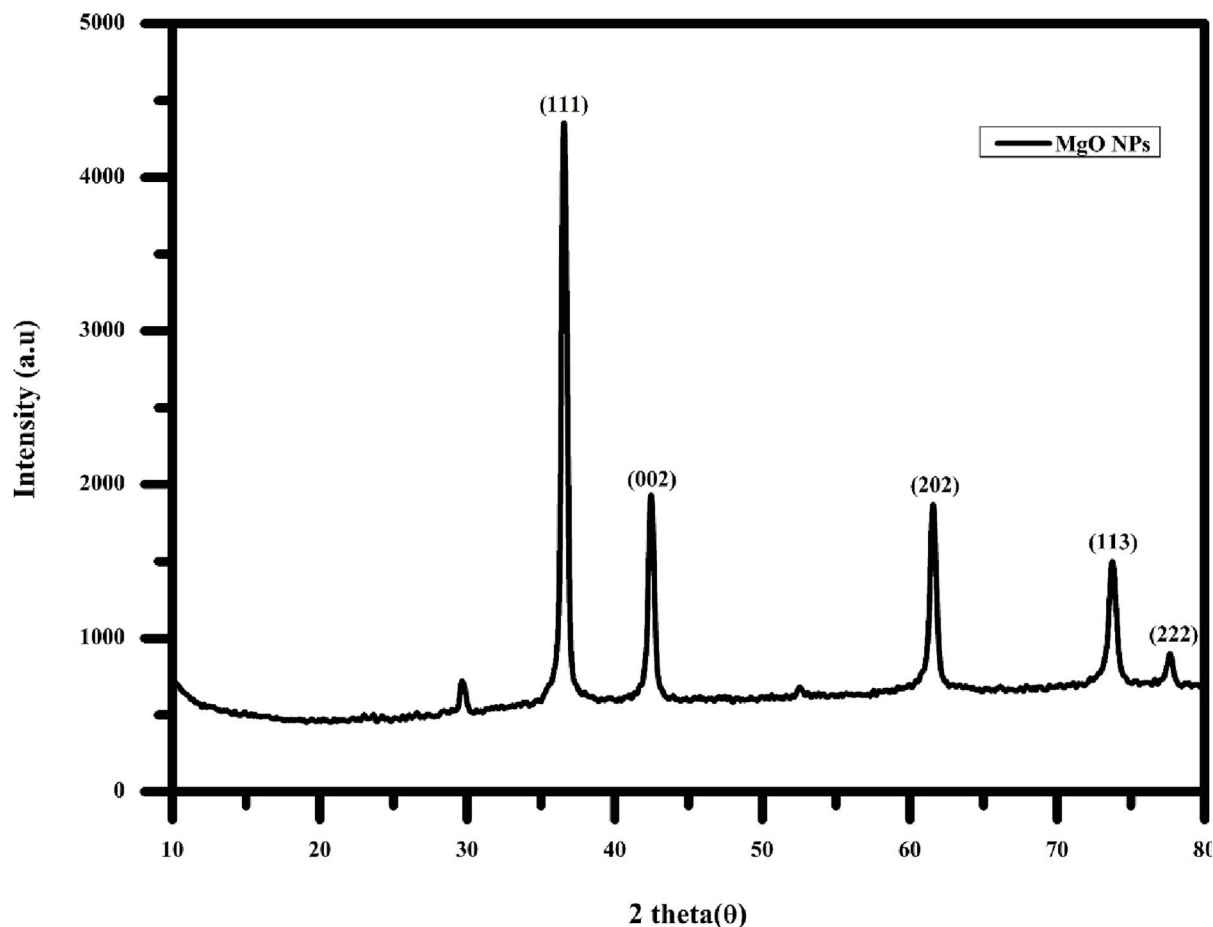
—WILEY

FIGURE 3 XRD spectrum of MgONPs.

with an atomic percentage of 58.92% and 48.92% (Figure 5). The formation of MgONPs was confirmed with the energy peak between 0.5 and 1.5 KeV.[65]

3.1.5 | Antibacterial assay

The minimum inhibitory concentration (MIC) was determined for five bacterial strains: *Bacillus subtilis*, *Escherichia coli*, *Staphylococcus aureus*, *Vibrio harveyi*, and *Vibrio parahaemolyticus* using biosynthesized MgONPs in the concentration ranging from 6, 3, 1.5, 0.75, and 0.375 μg/mL (Figure 6). The MIC of the MgONPs was 1.5 μg/mL. Growth of all the test bacteria was completely inhibited with the highest tested concentrations of 6 μg/mL. As the concentration of the drug reduced gradually, there was an increase in the growth of the microorganisms. NPs have been reported to be more susceptible to Gram-negative bacteria than Gram-positive bacteria, as the latter have a thick peptidoglycan layer, which acts as a barrier and prevents the entry of the nanoparticles.[66] The negative charge of the lipopolysaccharide in the Gram-negative cell wall facilitates the adhesion of the nanoparticles.[65] There are several mechanisms proposed

for the antibacterial effect of MgONPs. These NPs generate certain levels of H_2O_2, which induces oxidative stress in the cell. The interaction of NPs and cell surfaces disrupts the membrane integrity of bacteria.[67] The membrane damage causes leakage; thereby, irreversible oxidation of biomolecules (Proteins, DNA, lipids) occurs, leading to the cell's death.[68]

It has been proposed that NPs generated by using plant extract intercalate between the purine and pyrimidine and disrupt the hydrogen bond, thereby denaturing the DNA molecules.[69]

3.1.6 | In vitro cytotoxicity assay

In vitro cytotoxicity of MgONPs was assessed on the breast cancer (MCF-7) and Vero cells line (Figure 7). The IC_{50} of MgONPs was 113.56 and 785.69 μg/mL against MCF-7 and Vero cells respectively. This difference in toxicity may be due to the colloidal stability of the NPs. NPs infiltrate the cancer cells more efficiently than normal cells.[70] These NPs may accumulate in mitochondria and reduces the membrane potential, which interrupts ATP synthesis leading to the formation of high amounts of
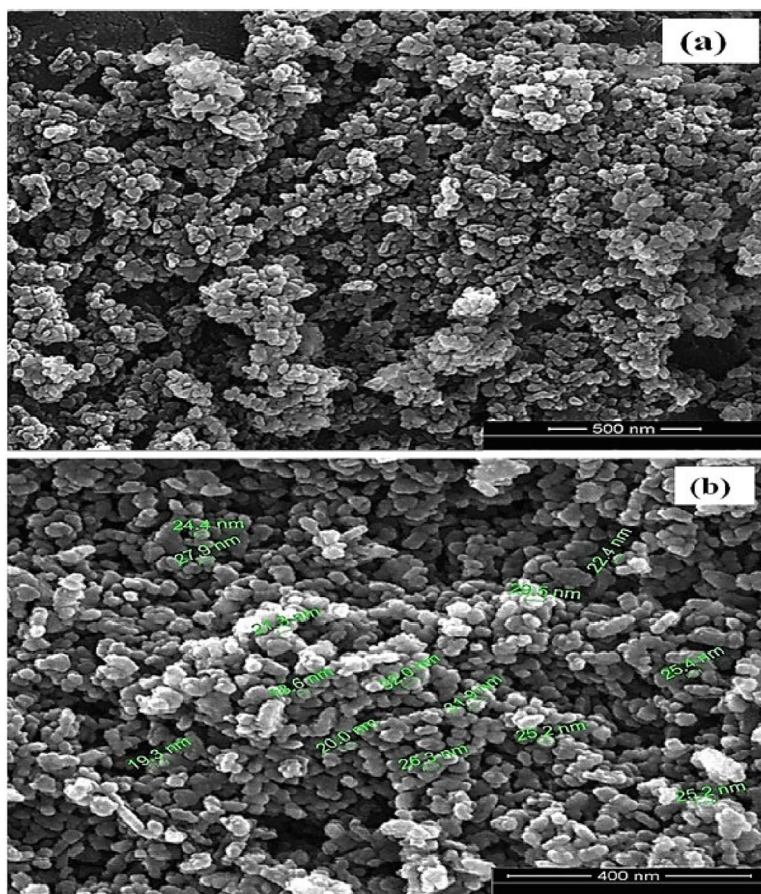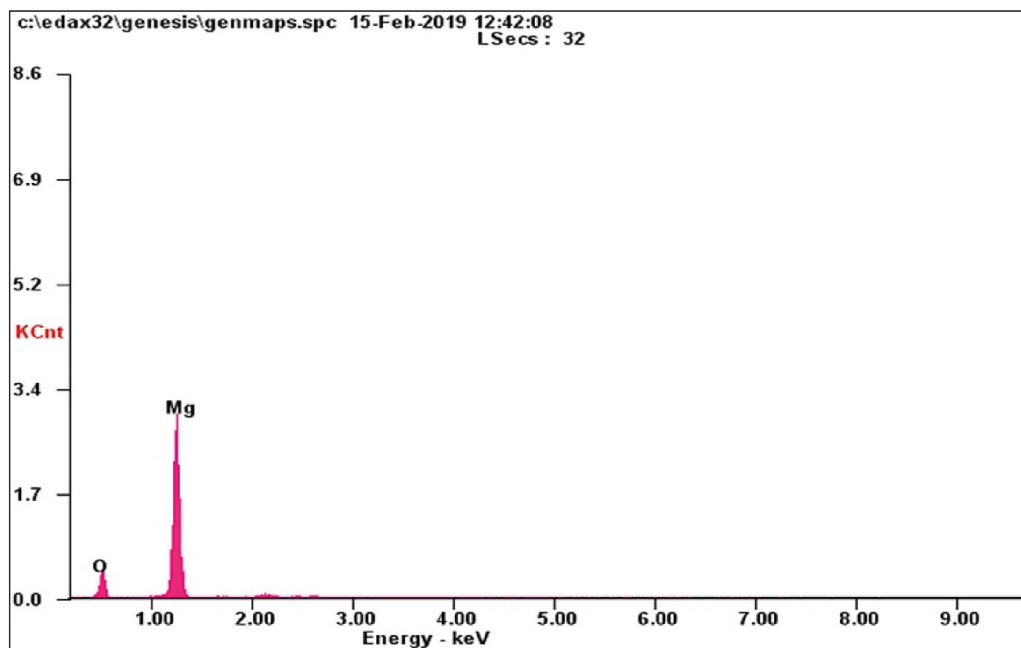
FIGURE 4 SEM micrograph of MgONPs.

FIGURE 5 EDX spectrum of MgONPs.

ROS.[20] ROS play an important role in cell death, which causes oxidative DNA damage by way of single and double-strand breaks, mutations, and generation of oxidized nucleotides.[71] The metal ions from nanoparticles play a key role in cytotoxicity.[72] NPs are internalized by nonspecific or specific endocytosis and remain in the cytoplasm or inside the intracellular vesicles. The ions released by the NPs may enter the nucleus and damage
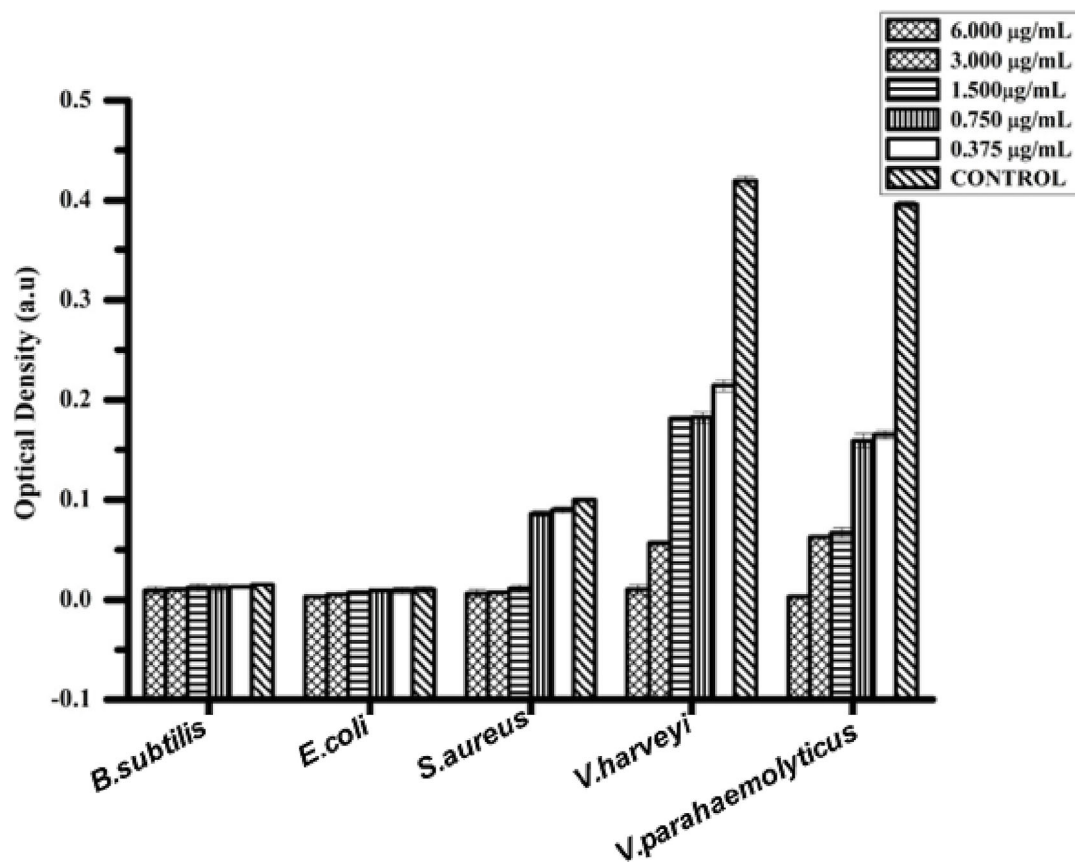
—WILEY

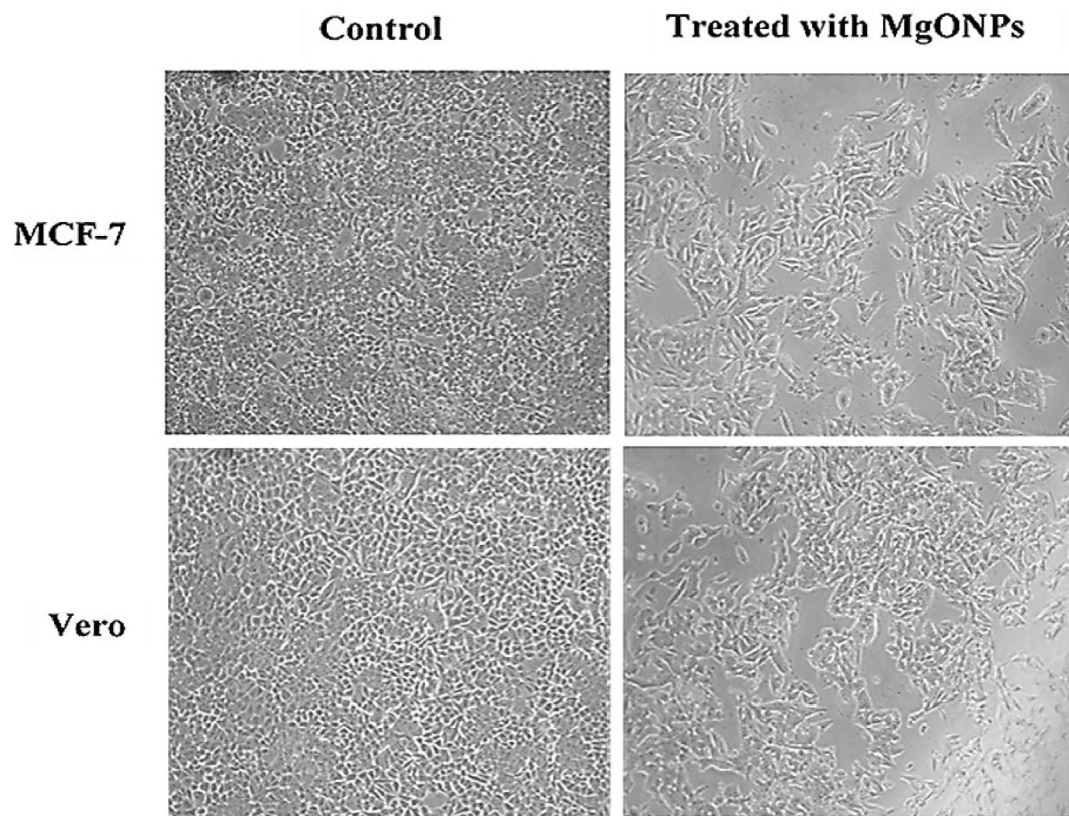**FIGURE 6** Antibacterial activity of MgONPs.

FIGURE 7 In vitro cytotoxicity of MgONPs on breast cancer cell line, MCF-7, and on normal Vero cell lines.

the DNA either by fragmentation or hypermethylation or arrest the cell cycle.[73] In vitro toxicological studies of MgONPs on human peripheral mononuclear cells (PBMC) showed no alternations in cell viability or membrane integrity. They had no cytotoxic effect on control cells, demonstrating its safety as a medicine.[74]

3.1.7 | In vitro hemolytic activity

The hemolytic assay revealed a dose-dependent effect of MgONPs on the red blood cells (RBCs) In vitro (Figure 8). The percentage of hemolysis at concentrations of 100, 50, 25, 12.5, 6.25, and 3.125 μg/mL was found to be 8.18%, 2.69%, 2.39%, 1.49%, and 1.19%, which indicates that as the concentration of the NPs increased the percentage of hemolysis increased.

The results show that hemolysis was directly proportional to the concentration of the NPs. According to the American Society for Testing Materials guidelines, the biocompatibility of compounds with >2% hemolysis are designated as no hemolytic, 2%–5% slightly hemolytic and >5% hemolytic.[75] The study proves that the synthesized MgONPs are non-toxic at the lowest tested concentration. The smaller size of NPs aids effective penetration into the cell; larger surface availability improves interaction and interferes with the cell's metabolism. Hemolysis occurs due to the size, surface chemistry, and physiochemical properties of the NPs. It is attributed to the reductive/oxidative process of interfacial charge interactions with RBCs.[76]

3.1.8 | Photocatalytic activity

The photocatalytic activity of MgONPs was studied by the degradation of methyl violet, Coomassie brilliant blue G-250, and malachite green (Figure 9a–c). At 60 min duration, the NPs showed the highest degradation of methyl violet by 96.12%, followed by Coomassie brilliant blue G-250 (95.13%) and malachite green (94.24%). Metal oxide NPs can absorb light and produce a charged separation that can oxidize or reduce organic compounds or dyes.[77,78] Light from the sun's irradiation can be absorbed by the catalyst and the dye molecule. Activation of MgONPs takes place on exposure to UV or visible
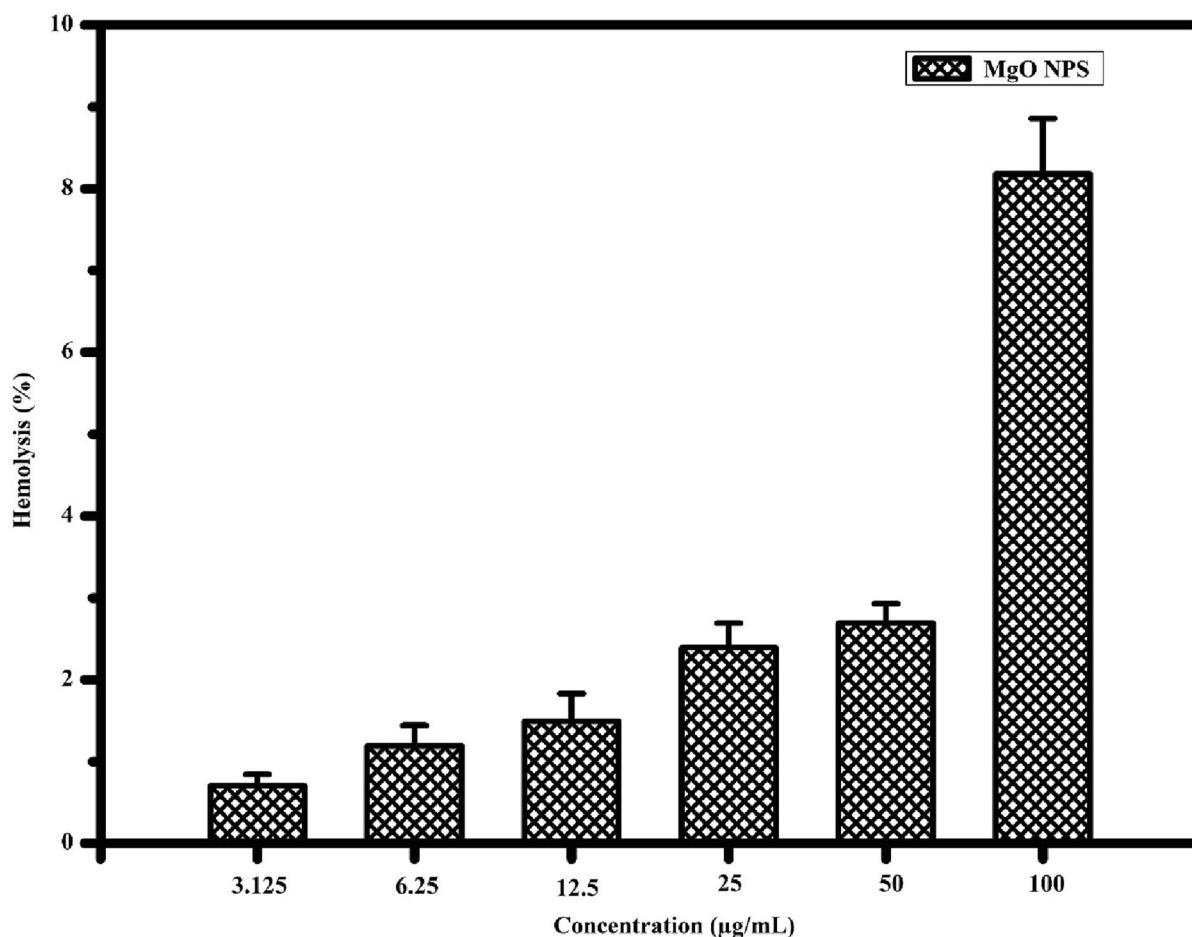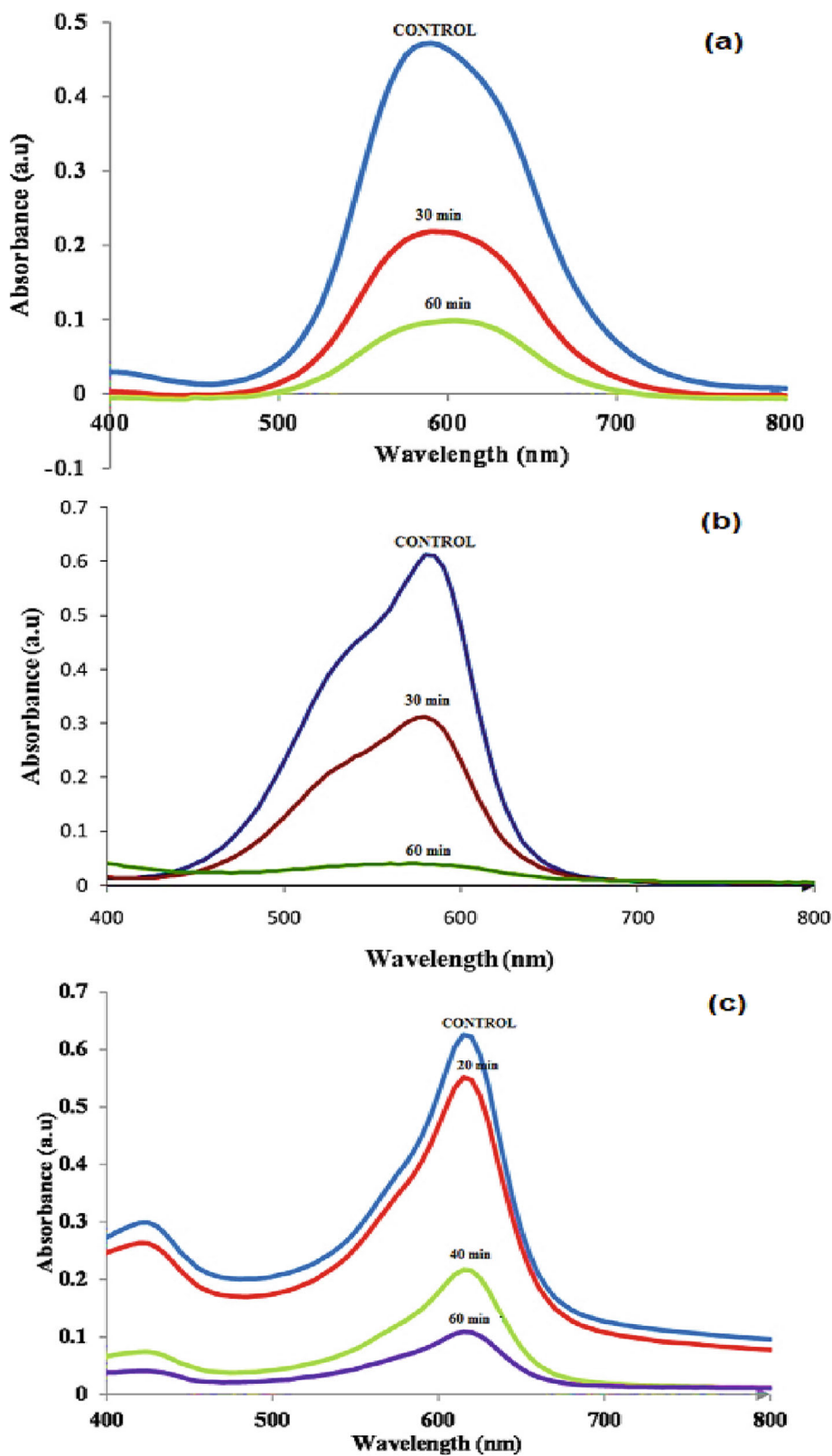

FIGURE 8 Percentage of RBC hemolysis by MgONPs.

FIGURE 9 Photo degradation of dye by MgONPs: (a) Coomassie brilliant blue, (b) methyl violet, (c) malachite green.

light; the photogenerated electrons are transferred from the valance band to the conduction banding. These electron/hole pairs (e−/h+) are responsible for the redox interaction of the adsorbed organic dyes on their surface.[1]

3.1.9 | Seed germination

The effect of the synthesized MgONPs was tested on the germination of *Vigna radiata*. At a test concentration of 10, 30, and 50 mg/mL, the length of the shoot (7–12 cm)
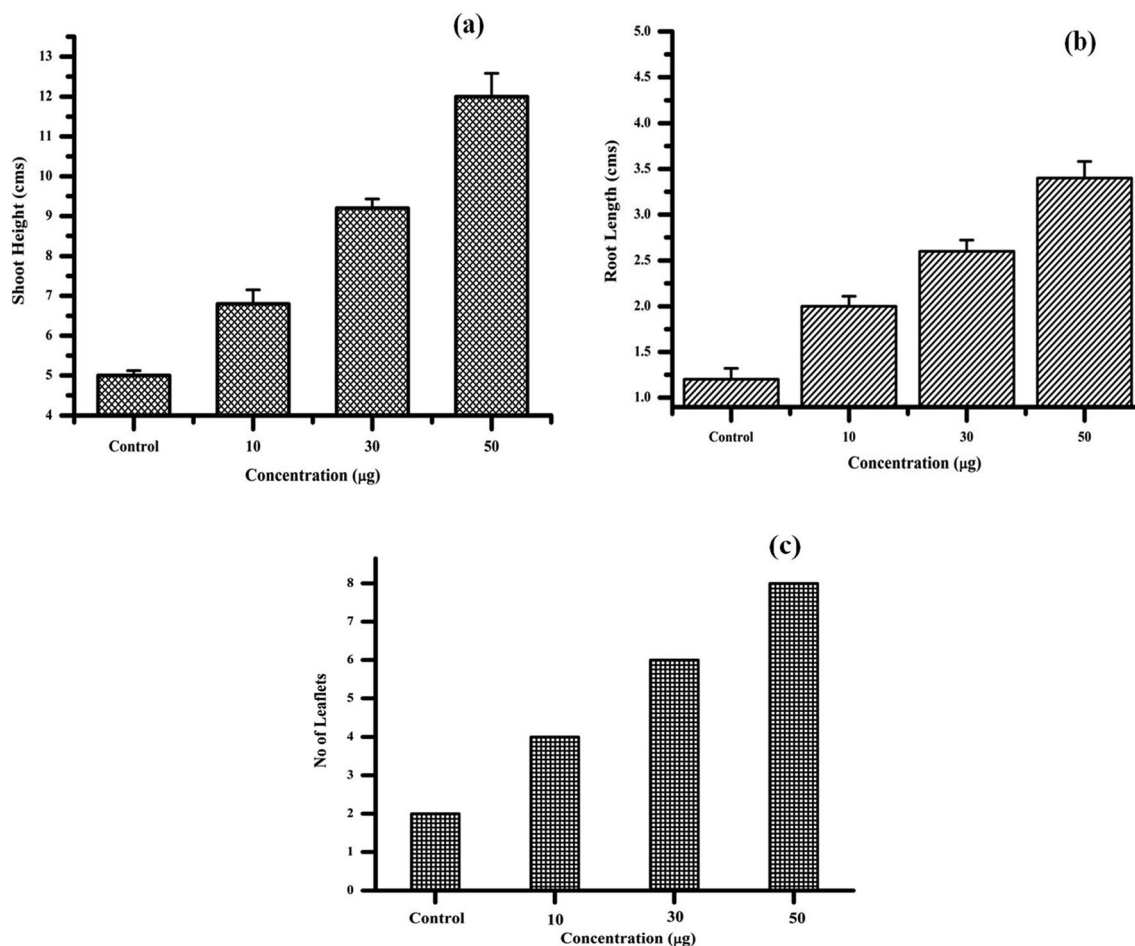
FIGURE 10   Seed germination by MgONPs. (a) Shoot length, (b) Root length, (c) No.of leaves.

and roots (2–3.5 cm) were enhanced compared with the control (Figure 10a,b). Leaf induction counts were more (4–8 leaflets per plant) as the concentration of the NPs increased (Figure 10c). Mg is a macronutrient essential for plant growth, and the ions play a major role in activating enzymes involved in seed germination.[79] NPs increase seeds′ water and nutrient absorption capacity by increasing the nitrate reductase enzyme level.[80] NPs may also help in the reduction of antioxidants stress of plants by reducing H_2O_2 and superoxide radicals and increasing the activity of superoxide dismutase, ascorbate peroxidase, guaiacol peroxidase, catalase, and so on.[81]

4 | CONCLUSION

The economic perspective and viability of green synthesis of NPs are of significant interest. This study reports the green synthesis of MgONPs using bract extract of *Musa acuminate* flower and their potential bioactivity. The size and morphology of the MgONPs confined the antibacterial targeting potential and the cytotoxicity. For the photodegradation of organic dyes in wastewater, MgONPs may prove to be a useful and versatile catalyst. The biogenic magnesium nanoparticles demonstrated good seed germination efficiency, indicating their potential to enter seed coat as a microelement source. To understand mechanism of its plant growth promotions, further extensive research is needed. Improving dependable metallic NP synthesis for commercial feasibility that is comparable with conventional methods would be a stride in applied nanotechnology.

AUTHOR CONTRIBUTIONS

Jayashree Shanmugam: Writing; editing; data analysis; validation. **Aruna Sharmili Sundararaj:** Concept; methodology; writing; editing; validation. **Roshitha Shanmugasundaram:** Methodology; investigation. **Balaji Ravichandran:** Investigation. **Mahendrakumar Mani:** Investigation. **Savaas Umar Mohammed Riyaz:** Data analysis. **Manikandan Dhayalan:** Concept; validation; review. **Antonio Cid-Samamed:** Investigation. **Jesus Simal-Gandara:** Concept; validation; review.

Applied Organometallic Chemistry—WILEY

DATA AVAILABILITY STATEMENT
Data are available on request from the authors.

ORCID
Jayashree Shanmugam https://orcid.org/0000-0001-6274-4943

Aruna Sharmili Sundararaj https://orcid.org/0000-0002-5774-804X

Roshitha Shanmugasundaram https://orcid.org/0000-0003-3394-7738

Balaji Ravichandran https://orcid.org/0000-0001-6023-6662

Mahendrakumar Mani https://orcid.org/0000-0003-4170-9246

Savaas Umar Mohammed Riyaz https://orcid.org/0000-0002-5306-8725

Manikandan Dhayalan https://orcid.org/0000-0001-6047-6850

Antonio Cid-Samamed https://orcid.org/0000-0002-0507-3394

Jesus Simal-Gandara https://orcid.org/0000-0001-9215-9737

REFERENCES

[1] M. Amina, N. M. Al Musayeib, N. A. Alarfaj, M. F. El-Tohamy, H. F. Oraby, G. A. Al Hamoud, S. I. Bukhari, N. M. Moubayed, *PLoS ONE* **2020**, *15*(8), e0237567.

[2] I. Khan, K. Saeed, I. Khan, *Nanoparticles: Arabian J. Chem.* **2019**, *12*(7), 908.

[3] A.A Sorescu, A. Nuă, R. M. Ion, Ş. B. Ioana-Raluca, Proceedings of The 4th International Virtual Conference on Advanced Scientific Results. **2016**.

[4] P. Makvandi, M. Ghomi, V. V. Padil, F. Shalchy, M. Ashrafizadeh, S. Askarinejad, N. Pourreza, A. Zarrabi, N. E. Zare, M. Kooti, B. Mokhtari, A. Borzacchiello, F. R. Tay, *ACS Appl. Nano Mat.* **2020a**, *3*(7), 6210.

[5] P. Makvandi, C. Wang, E. N. Zare, A. Borzacchiello, L. Niu, F. R. Tay, *Adv. Functional Mat.* **2020b**, *30*(22), 1910021.

[6] S. Ahmed, M. Ahmad, B. L. Swami, S. Ikram, *J. Adv. Res.* **2016**, *7*(1), 17.

[7] R. Vijayan, S. Joseph, B. Mathew, *Artificial Cells Nanomed. Biotech.* **2017**, *46*(4), 861.

[8] S. Abinaya, H. P. Kavitha, M. Prakash, A. Muthukrishnaraj, *Sustain. Chem. Pharm.* **2021**, *9*, 100368.

[9] M. A. Ammulu, V. K. Viswanath, A. K. Giduturi, P. K. Vemuri, U. Mangamuri, S. Poda, *J. Genetic Eng. Biotech.* **2021**, *19*, 1.

[10] M. I. Khan, M. N. Akhtar, N. Ashraf, J. Najeeb, H. Munir, T. I. Awan, M. B. Tahir, M. R. Kabli, *Appl. Nanoscience.* **2020**, *10*(7), 2351.

[11] C. Vanlalveni, S. Lallianrawna, A. Biswas, M. Selvaraj, B. Changmai, S. L. Rokhum, *RSC Adv.* **2021**, *11*(5), 804.

[12] G. Sharma, J. S. Nam, A. Sharma, S. S. Lee, *Molecules* **2018**, *23*(9), 2268.

[13] B. Changmai, I. B. Laskar, L. Rokhum, *J. Taiwan Inst. Chem. Eng.* **2019**, *02*, 276.

[14] M. Bandeira, M. Giovanela, M. Roesch-Ely, D. M. Devine, J. Crespo, S. da, *Sustain. Chem. Pharm.* **2020**, *15*(6), 100223.

[15] B. Mahdavi, S. Saneei, M. Qorbani, M. Zhaleh, A. Zangeneh, M. M. Zangeneh, E. Pirabbasi, N. Abbasi, H. Ghaneialvar, *Appl. Organomet. Chem.* **2019**, *33*(11), e5164.

[16] M. Hassanisaadi, A. H. S. Bonjar, A. Rahdar, R. S. Varma, N. Ajalli, S. Pandey, *Materials Today Communications.* **2022**, *33*, 104183.

[17] S. Ahmed, S. A. C. Annu, S. Ikram, *J. Photochem. Photobiol. B: Biol.* **2017**, *166*, 272. https://doi.org/10.1016/j.jphotobiol.2016.12.011

[18] G. A. Naikoo, M. Mustaqeem, I. U. Hassan, T. Awan, F. Arshad, H. Salim, A. Qurashi, *J. Saudi Chem. Soc.* **2021**, *25*(9), 101304.

[19] R. B. Singh, V. Kshitij, J. Nayak, A. K. Singh, R. P. Singh, *RSC Adv.* **2021a**, *11*(40), 24722.

[20] M. M. Zangeneh, S. Saneei, A. Zangeneh, R. Toushmalani, A. Haddadi, M. Almasi, A. Amiri-Paryan, *Appl. Organomet. Chem.* **2019**, *33*(11), e5216.

[21] G. A. Rather, A. Nanda, P. Ezhumalai, *J. Nanostruct.* **2022**, *12*(3), 625.

[22] T. H. Duong, T. N. Nguyen, H. T. Oanh, T. A. D. Thi, L. N. Giang, H. T. Phuong, N. T. Anh, B. M. Nguyen, V. T. Quang, G. T. Le, T. V. Nguyen, *J. Chem.* **2019**, *2019*, 1.

[23] A. Jain, S. Wadhawan, V. Kumar, S. K. Mehta, *Chem. Phys. Lett.* **2018**, *706*, 53.

[24] A. Singh, N. C. Joshi, M. Ramola, *Res. J. Pharm. Tech.* **2019**, *12*(10), 4644.

[25] R. Ali, Z. Shanan, G. M. Saleh, Q. Abass, *Iraqi J. Sci.* **2020**, 266.

[26] B. Mangalampalli, N. Dumala, P. Grover, *J. Environ. Sci.* **2018**, *66*, 125.

[27] Y. Cai, C. Li, D. Wu, W. Wang, F. Tan, X. Wang, P. K. Wong, X. Qiao, *Chem. Eng. J.* **2017**, *312*, 158.

[28] S. Jorfi, G. Barzegar, M. Ahmadi, R. D. C. Soltani, A. N. J. Haghighifard, A. Takdastan, R. Saeedi, M. Abtahi, *J. Environ. Manage.* **2016**, *177*, 111.

[29] M. Fernandes, K. R. B. Singh, T. Sarkar, P. Singh, R. P. Singh, *Adv. Mater. Let.* **2020**, *11*(8), 1.

[30] A. Khalid, R. Norello, N. A. Abraham, J. P. Tetienne, T. J. Karle, E. W. C. Lui, K. Xia, P. A. Tran, J. A. O'Connor, B. G. Mann, R. de Boer, Y. He, A. M. C. Ng, A. B. Djurisic, R. Shukla, S. Tomljenovic-Hanic, *Nanomat* **2019**, *9*(10), 1360.

[31] N. Y. T. Nguyen, N. Grelling, C. L. Wetteland, R. Rosario, H. Liu, *Sci. Rep.* **2018**, *8*, 1.

[32] A. Pugazhendhi, R. Prabhu, K. Muruganantham, R. Shanmuganathan, S. Natarajan, *J. Photochem. Photobiol. B: Biol.* **2019**, *195*(67), 86.

[33] M. J. Akhtar, M. Ahamed, H. A. Alhadlaq, S. A. Alrokayan, *J. Trace Elem. Med. Biol.* **2018**, *50*, 283.

10990739, 2023, 5, Downloaded from https://onlinelibrary.wiley.com/doi/10.1002/aoc.7063 by Universidad de Vigo, Wiley Online Library on [26/10/2023]. See the Terms and Conditions (https://onlinelibrary.wiley.com/terms-and-conditions) on Wiley Online Library for rules of use; OA articles are governed by the applicable Creative Commons License

[34] D. R. Di, Z. Z. He, Z. Q. Sun, J. Liu, *Nanomedicine: Nanotech. Biol. Medicine.* **2012**, *8*(8), 1233.

[35] E. Behzadi, R. Sarsharzadeh, M. Nouri, F. Attar, K. Akhtari, K. Shahpasand, M. Falahati, *Int. J. Nanomedicine* **2019**, *14*, 257.

[36] S. V. Sudakaran, J. R. Venugopal, G. Puvala, *Mat. Sci. Eng.* **2017**, *C71*, 620.

[37] S. K. Moorthy, C. Ashok, K. V. Rao, C. Viswanathan, *Mat. Today: Proceedings.* **2015**, *2*, 4360.

[38] L. Umaralikhan, M. J. M. Jaffar, Iranian J Sci Tech, Transactions A: Science, **2018**, *42*, 477.

[39] Y. Abdallah, S. O. Ogunyemi, A. Abdelazez, M. Zhang, X. Hong, E. Ibrahim, A. Hossain, H. Fouad, B. Li, J. Chen, *BioMed Res. Int.* **2019**, 5620989.

[40] E. R. Essien, V. N. Atasie, A. O. Okeafor, D. O. Nwude, *Int. Nano. Letters.* **2020**, *10*, 43.

[41] H. Dabhane, S. Ghotekar, M. Zate, S. Kute, G. Jadhav, V. Medhane, *Inorganic Chem. Communications.* **2022**, *138*, 109270.

[42] S. A. Kumar, M. Jarvin, S. S. R. Inbanathan, A. Umar, N. P. Lalla, N. Y. Dzade, H. Algadi, Q. I. Rahman, S. Baskoutas, *Environmental Tech. & Innovation.* **2022**, *28*, 102746.

[43] A. D'Hont, F. Denoeud, J. M. Aury, F. C. Baurens, F. Carreel, O. Garsmeur, B. Noel, S. Bocs, G. Droc, M. Rouard, C. Da Silva, K. Jabbari, C. Cardi, J. Poulain, M. Souquet, K. Labadie, C. Jourda, J. Lengellé, M. Rodier-Goud, A. Alberti, M. Bernard, M. Correa, S. Ayyampalayam, M. R. Mckain, J. Leebens-Mack, D. Burgess, M. Freeling, D. Mbéguié-A-Mbéguié, M. Chabannes, T. Wicker, O. Panaud, J. Barbosa, E. Hribova, P. Heslop-Harrison, R. Habas, R. Rivallan, P. Francois, C. Poiron, A. Kilian, D. Burthia, C. Jenny, F. Bakry, S. Brown, V. Guignon, G. Kema, M. Dita, C. Waalwijk, S. Joseph, A. Dievart, O. Jaillon, J. Leclercq, X. Argout, E. Lyons, A. Almeida, M. Jeridi, J. Dolezel, N. Roux, A. -Ma Risterucci, J. Weissenbach, M. Ruiz, J.-C. Glaszmann, F. Quétier, N. Yahiaoui, P. Wincker, *Nature* **2012**, *488*(7410), 213.

[44] R. S. Prasanth, D. Kumar, A. Jayalakshmi, G. Singaravelu, K. Govindaraju, K. V. Ganesh, *Indian J. Geo Marine Sci.* **2019**, *48*(08), 1210.

[45] S. K. Moorthy, C. H. Ashok, K. V. Rao, C. Viswanathan, *Materials Today: Proceedings.* **2015**, *2*(9), 4360.

[46] T. A. Saleh, K. O. Sulaiman, S. A. AL-Hammadi, H. Dafalla, G. I. Danmaliki, *J. Clean. Prod.* **2017**, *154*, 401.

[47] P. Premasudha, M. Venkataramana, M. Abirami, P. Vanathi, K. Krishna, R. Rajendran, *Bull. Mat. Sci.* **2015**, *38*(4), 965.

[48] M. Rajapriya, S. A. Sharmili, R. Baskar, R. Balaji, N. S. Alharbi, S. Kadaikunnan, J. M. Khaled, K. F. Alanzi, B. Vaseeharan, *J. Cluster Sci.* **2019**, *31*(4), 791.

[49] T. Muthukumarasamyvel, R. Baskar, S. Chandirasekar, K. Umamaheswari, N. Rajendiran, *ACS Appl. Mater. Interfaces* **2016**, *8*(38), 25111.

[50] S. Roshitha, V. Mithra, V. Saravannan, S. S. Kumar, M. Gnanadesigan, *Biores. Tech. Reports.* **2018**, *5*, 339.

[51] A. Umamaheswari, A. Puratchikody, S. L. Prabu, T. Jayapriya, *Int. Res. J. Pharmacy.* **2017**, *8*(8), 41.

[52] P. R. Hemlata, A. P. Meena, K. K. Singh, *Tejavath, ACS Omega* **2020**, *5*(10), 5520.

[53] A. Es-haghi, M. E. T. Yazdi, M. Sharifalhoseini, M. Baghani, E. Yousefi, A. Rahdar, F. Baino, *Biomimetics.* **2021**, *6*, 34.

[54] P. Singh, K. R. B. Singh, J. Singh, P. Prasad, R. P. Singh, *RSC Adv.* **2021b**, *11*(41), 25752.

[55] S. Pirtarighat, M. Ghannadnia, S. Baghshahi, *J. Nanostructure Chem.* **2018**, *9*(1), 1.

[56] N. Liaqat, N. Jahan, T. Khalil-ur-Rahman, H. Q. Anwar, *Front. Chem.* **2022**, *10*, 952006.

[57] J. Jeevanandam, Y. S. Chan, M. K. Danquah, *New J. Chem.* **2017**, *41*(7), 2800.

[58] V. Mohammadzadeh, M. Barani, M. S. Amiri, M. E. Taghavizadeh, M. Hassanisaadi, A. Rahdar, R. S. Varma, *Sustain. Chem. Pharm.* **2022**, *25*, 100606.

[59] A. K. Sidhu, N. Verma, P. Kaushal, *Frontiers in Nanotech* **2022**, *3*, 3.

[60] R. Javed, M. Zia, S. Naz, S. O. Aisida, N. U. Ain, Q. Ao, *J. Nanobiotech.* **2020**, *18*, 1.

[61] H. Fissan, S. Ristig, H. Kaminski, C. Asbach, M. Epple, *Anal. Methods* **2014**, *6*(18), 7324.

[62] G. Balakrishnan, R. Velavan, K. M. Batoo, E. H. Raslan, *Results Phys.* **2020**, *16*, 103013.

[63] S. Balamurugan, L. Ashna, P. Parthiban, *J. Nanotech.* **2014**, *2014*, 1.

[64] J. Huang, L. Lin, Q. Li, D. Sun, Y. Wang, Y. Lu, N. He, K. Yang, X. Yang, H. Wang, W. Wang, W. Lin, *Industrial & Eng. Chem. Res.* **2008**, *47*(16), 6081.

[65] R. Dobrucka, *Iranian J. Sci. Tech. Trans. A: Sci.* **2016**, *42*(2), 547.

[66] A. G. Femi-Adepoju, A. O. Dada, K. O. Otun, A. O. Adepoju, O. P. Fatoba, *Heliyon.* **2019**, *5*, e01543.

[67] M. K. Choudhary, J. Kataria, S. Sharma, *Appl. Nanosci.* **2017**, *7*(7), 439.

[68] V. Gopinath, S. Priyadarshini, M. F. Loke, J. Arunkumar, E. Marsili, D. M. Ali, P. Velusamy, J. Vadivelu, *Arabian J. Chem.* **2017**, *10*(8), 1107.

[69] A. M. Pillai, V. S. Sivasankarapillai, A. Rahdar, J. Joseph, F. Sadeghfar, F. Sadeghfar, A. R. Anuf, A. K. Rajesh, Z. G. Kyzas, *J. Mol. Struct.* **2020**, *1211*, 128107.

[70] Y. He, S. Ingudam, S. Reed, A. Gehring, T. P. Strobaugh, P. Irwin, *J. Nanobiotech.* **2016**, *14*, 1.

[71] N. Bertrand, J. Wu, X. Xu, N. Kamaly, O. C. Farokhzad, *Adv. Drug Deliv. Rev.* **2014**, *66*, 2.

[72] A. Pugazhendhi, R. Prabhu, K. Muruganantham, R. Shanmuganathan, S. Natarajan, *J. Photochem. Photobiol. B: Biol.* **2019**, *190*, 86.

[73] A. Grzelak, M. Wojewódzka, S. Meczynska-Wielgosz, M. Zuberek, D. Wojciechowska, M. Kruszewski, *Redox Biol.* **2018**, *15*, 435.

[74] J. Shanmugam, M. Dhayalan, M. R. Savaas Umar, M. Gopal, M. Ali Khan, J. Simal-Gandara, A. Cid-Samamed, *Nanomaterials* **2022**, *12*(10), 1725.

[75] P. Sathishkumar, J. Preethi, R. Vijayan, A. R. M. Yusoff, F. Ameen, S. Suresh, R. Balagurunathan, T. Palvannan, *J. Photochem. Photobiol. B: Biol.* **2016**, *163*, 69.

[76] M. Grijalva, M. J. Vallejo-López, L. Salazar, J. Camacho, B. Kumar, **2018**.

[77] M. Q. Nasar, A. T. Khalil, M. Ali, M. Shah, M. Ayaz, Z. K. Shinwari, *Medicina* **2019**, *55*(7), 369.

[78] C. Ashokraja, M. Sakar, S. Balakumar, *Mat. Res. Express.* **2017**, *4*(10), 105406.

[79] T. Hisatomi, J. Kubota, K. Domen, *Chem. Soc. Rev.* **2014**, *43*(22), 7520.

[80] M. R. Hoffmann, S. T. Martin, W. Choi, D. W. Bahnemann, *Chem. Rev.* **1995**, *95*(1), 69.

[81] S. Shinde, P. Paralikar, A. P. Ingle, M. Rai, *Arabian J. Chem.* **2020**, *13*(1), 3172.